ELSEVIER

Journal of Hydrology 187 (1996) 3–27

Journal of Hydrology

Energy decomposition of rainfall in the time–frequency–scale domain using wavelet packets

V. Venugopal, E. Foufoula-Georgiou*

St. Anthony Falls Laboratory, Department of Civil Engineering, University of Minnesota, Minneapolis, MN 55414, USA

Received 11 December 1995; accepted 30 January 1996

Abstract

The time–frequency–scale features of high-resolution rainfall are investigated in an effort to gain more insight into the rainfall-generating mechanism. In particular, we look for the existence of persistent and short-lived structures and their associated frequencies and time (length) scales, as well as the energy they carry. We try to achieve this objective via the wavelet packet representation. The best representation for a signal from the point of view of minimum entropy (i.e. maximum information in a few coefficients) is obtained, and, in the process, we define two measures: (1) best basis spectrum, which is analogous to the well-known Fourier spectrum; (2) frequency persistence spectrum, a new measure, which in essence gives an idea of what scale has been chosen to best represent a particular frequency; thus the localization of that frequency in time, whether persistent or short lived, is known. We discuss the implications of our analysis in separating stratiform and convective components of rain and in gaining insight into the rainfall energy cascading mechanism for the purpose of model building.

1. Introduction

Rainfall, being the result of complex atmospheric phenomena, possesses a complicated temporal and spatial structure. A wide range of frequency–content features and extreme variability over time intervals from a few seconds to years make rainfall an intriguing and challenging process to study. The temporal structure of rainfall at a point has been the subject of intense study over the past two decades.

Markovian-type structures for hourly and daily rainfall formed the core of early models used to explain rainfall's extreme variability (e.g. Gabriel and Neumann, 1962). The

* Corresponding author.

PII S0022-1694(96)03084-3

structure and the parameters of these models depended heavily on the time scale chosen for representing the rainfall process. This limitation led to the formulation of continuous-time conceptual rainfall models, which would be applicable over several time scales (e.g. see Waymire et al., 1984). The hope was that this continuous-time rainfall parameterization would shed light on the underlying rainfall-generating mechanism. However, although these were valid simulation models, they fell short in providing a good understanding of the underlying structure of the rainfall process. A major drawback was that there were too many parameters embedded in the model structure, resulting in non-uniqueness and non-identifiability problems when the models were fitted to rainfall observations at different scales (e.g. see Foufoula-Georgiou and Guttorp, 1987).

The fact that rainfall exhibits considerable variability over scales of the order of seconds makes it all the more important and exciting to study the rainfall phenomenon at such fine scales. However, lack of data has made impossible such fine-scale studies until recently, when some high-resolution data have become available.

A recent analysis of high-resolution temporal data by Olsson et al. (1993) suggested that rainfall intensities show scaling. Olsson et al. analyzed six 1 min rainfall data sets (which spanned 2 years) to obtain scale-invariant properties of temporal rainfall. They claimed that their results, obtained by the box counting method, indicate simple scaling with three different scaling exponents over three different ranges of scales. The two breaks in scaling correspond, as expected, to the storm duration and inter-arrival time of the storms.

Spectral analysis was performed by Georgakakos et al. (1994) on seven high-resolution temporal data (5 s intervals) collected at the Iowa Institute of Hydraulic Research (IIHR). These workers claimed that scaling exists over short time scales (up to a few tens of seconds) and a break in scaling occurs towards larger time scales. They also claimed that 'for a considerably larger sample of such long storms, ... it is probable that scale invariance holds in the high-frequency range, if at all'. Again, they mentioned this with an element of caution, as in the high-frequency range, the properties of the sensor measurement error and the properties of the process under consideration become indistinguishable and what needs to be hoped for is that the scale invariance is in fact a true feature of the phenomenon (rainfall in our case) and not of the measurement process. Georgakakos et al. also studied the behavior of the exceedance probabilities, and reported an intermittency parameter γ (which is a measure of the linearity in decay of the tail of the exceedance probability distribution (log–log plot) of the fluctuations of the process under study) for four of the rainfall data sets, in the range of 1.7–2.9.

This paper deals with an investigation of time–frequency–scale features of high-resolution temporal rainfall. In particular, we look for the existence of persistent and short-lived structures and their associated frequencies and time (length) scales. Although it is not clear at this time what the typical 'objects' or 'elementary structures' that compose a rainfall field are, recent evidence of scaling, energy cascading and similarity to fully developed turbulence, and earlier observations about the existence of hierarchical structures in rainfall (see, e.g. Lovejoy and Schertzer, 1990; Gupta and Waymire, 1990; Kumar and Foufoula-Georgiou, 1993a, b), point to the presence of an organized structure that needs to be localized in both time (space) and frequency, to yield meaningful information. For instance, the cascade models in turbulence, which have recently been used for rainfall modeling, assume that wavenumber octaves are the elementary objects in homogeneous

turbulence and that their interactions consist of changing energy with neighboring octaves. More recent evidence (e.g. see Farge et al., 1992; Wickerhauser et al., 1994) suggests that cascading of energy in turbulent flows takes place only locally within coherent structures, and that only a limited active portion of the vorticity field, related to coherent structures, is responsible for the turbulent cascades.

A systematic approach to determine what kind of 'objects' exist in a field is to find an appropriate segmentation of energy density in the phase-space (energy as a function of time, frequency and scale) and to define phase-space 'atoms', among which energy or any dynamically relevant quantity is distributed and exchanged by the flow dynamics of the rainfall fields. It is worth stressing here again the issue of extreme variability of rainfall, in the sense that rainfall exhibits a high degree of intermittency, and thus arises the need for studying the time-localization of such a behaviour. This is the scope of this research, and the tool that has been chosen for this analysis is wavelet packets. Before we delve into the merits of a wavelet packet representation for temporal rainfall analysis, we define time–frequency tiling and discuss the underlying idea of a time–frequency–scale representation.

The time–frequency plane is a plane defined by time which spans the signal's time domain, or part of it as necessary, and frequency which ranges from zero to the Nyquist frequency (i.e. $1/2\delta$, where δ is the sampling interval). The idea of a time–frequency analysis is to 'tile' this plane (also termed phase-space) with rectangles and assign to each rectangle a magnitude representing the energy of the signal in the time–frequency interval spanned by the rectangle. The way the tiling of the plane is done depends on the basis chosen to represent the signal. Let us consider a rectangle centered around the point (t_0,ω_0) as shown in Fig. 1. The width of the rectangle in each direction represents the uncertainty with which the frequency ω_0 or time t_0 can be resolved. Heisenberg's uncertainty principle dictates that σ_ω and σ_t, the uncertainties in frequency and time, cannot be simultaneously made arbitrarily small. Thus, if the plane were to be tiled with thin tall boxes, we would have a very good time localization and no frequency localization. This is the case with a standard basis, where the signal is represented as a superposition of Dirac deltas. At the other extreme, if we decide to tile the plane with wide and short boxes, this is

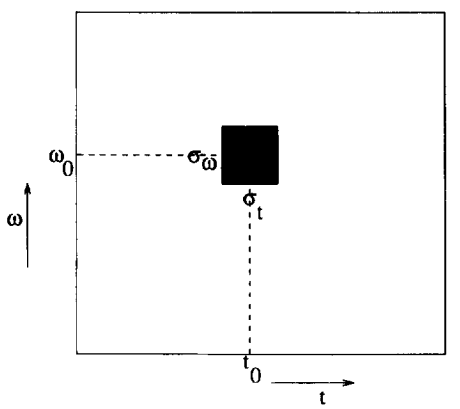

Fig. 1. Time–frequency tiling.

equivalent to a Fourier representation, wherein there is optimal frequency localization and no time localization. The tiling of the time–frequency plane is dependent on what information one needs to extract and also on a priori knowledge of the signal. To characterize a signal by being able to associate various frequency bands with different time intervals is called time–frequency analysis (tiling/localization). Now that we have seen what time–frequency analysis is, we try to compare the advantages and disadvantages of three bases which have proved to be useful in their own right.

As is well known, Fourier transforms provide no time localization of the frequencies present in the signal (sinusoids have infinite support in time). However, using wavelet representations, one can obtain good time localization owing to the fact that wavelets are compactly supported. Despite their ability to provide 'good' time–frequency localization, in terms of capturing optimal time–frequency features of the process under consideration, wavelet transforms (and, naturally, Fourier representations too) suffer from an inherent drawback: the basis is decided beforehand (once the wavelet is chosen) and hence is not a data-adaptive basis. Also, in wavelet transforms, every scale is spanned by a one-period wave, i.e. scale = (frequency)$^{-1}$, when, in fact, a process under study might contain persistent structures, i.e. structures which span a length scale greater than the period of the waves best describing the frequency content of this structure. This drawback is overcome by wavelet packets, which encompass a family of orthonormal bases, from which a data-adaptive basis can be chosen by minimizing an objective function such as entropy (the basis so obtained is given the name best basis). In fact, in the wavelet packet case, scale $\neq$ (frequency)$^{-1}$, i.e. every scale is spanned by multiple period waves (from one-period wave to Nyquist-period waves). The partition of the time–frequency plane by the wavelet packet best basis provides information on how much energy is present in a frequency band and over scales that best represent that frequency band. Wavelet packets have been successfully applied in a variety of fields, notably: (1) compression of data and identification of coherent structures in two-dimensional turbulent flows (Farge et al., 1992): (2) classifying and characterizing signals, and, in particular, extracting geological information from acoustic waveforms (Saito, 1994); (3) time–frequency analysis (in particular, presence of persistent structures) of temporal rainfall (Venugopal, 1995); (4) very recently, identification of coherent structures in temporal rainfall (Kumar, 1996).

This paper is arranged as follows. Section 2 presents a brief summary of the theory behind wavelets and wavelet packets. We then define two measures to interpret the time–frequency plots. Section 3 presents the results of our investigation of the time–frequency characteristics of high-resolution temporal rainfall when represented using the wavelet packet best basis. Finally, Section 4 presents conclusions and directions for future research.

2. An overview of wavelets and wavelet packets

Families of functions of the form

$$\psi^{a,b}(t) = \frac{1}{\sqrt{|a|}}\,\psi\left(\frac{t-b}{a}\right), \quad a>0, \quad b\in R \tag{1}$$

generated from one function ψ by translations and dilations, are called wavelets. ψ in Eq. (1) is called the 'mother wavelet', and a and b are the dilation (scaling) and translation (location) parameters, respectively. The factor $\frac{1}{\sqrt{|a|}}$ is a normalization factor chosen to ensure that the L^2 norm of the wavelet is unity.

The continuous wavelet transform (CWT) of a function f is defined as

$$W_\psi f(a,b) = |a|^{-1/2} \int f(t)\psi\left(\frac{t-b}{a}\right)dt \tag{2}$$

The mother wavelet is chosen to have the following properties: (1) compact support, to facilitate time localization; (2) zero mean, to permit reconstruction.

The discretization of the scale parameter a and the location parameter b leads to the discrete wavelet transform. If the discretization is chosen as $a = a_0^m$ and $b = nb_0a_0^m$, then the discrete wavelet transform is given as

$$DW_\psi f(m,n) = |a_0|^{-m/2} \int f(t)\psi(a_0^{-m}t - nb_0)dt \tag{3}$$

For $a_0 = 2$, $b_0 = 1$, it can be shown that an orthonormal family of functions can be constructed (Daubechies, 1992) and the wavelet representation can be seen in a multi-resolution framework by introducing a new function called the scaling function, denoted by $\phi(t)$ (for more details see Mallat (1989a,b)).

From a filtering point of view, the convolution of the signal (function) with the scaling function can be seen as a low-pass filtering and convolution with the wavelet can be seen as a high-pass filtering (the latter is evident from the fact that wavelet is a band-pass filter, as $\hat{\psi}(0) = 0$). Towards this end, the wavelet decomposition can be seen as a repeated convolution of the low-pass output with two sets of coefficients $\{c_k\}$ and $\{d_k\}$, representing convolution with the scaling function and the wavelet, respectively. From a time–frequency point of view, each stage of the decomposition can be visualized as an improvement of frequency resolution (low-frequency bands) in the frequency domain (direction) and a corresponding loss of time resolution (owing to Heisenberg's uncertainty principle), and is depicted in Fig. 2.

In the wavelet decomposition case, only the low-frequency bands are decomposed. We go a step further in obtaining a more generic decomposition (representation) by decomposing the high-frequency bands also. The interesting aspect is that, by using a combination of $\{c_k\}$ and $\{d_k\}$ to produce two-scale relations with ψ, the wavelet spaces, W_n, can be further decomposed orthogonally. The sequence of functions thus obtained are called 'wavelet packets'. A wavelet packet is defined as a square integrable modulated waveform, well localized in both position and frequency (Wickerhauser, 1991). The ensuing representation has come to be known as the wavelet packet representation. An informative picture is a tree of the wavelet packet coefficients. For instance, the computation of such a tree for a signal with eight points is shown in Fig. 3 (Wickerhauser, 1991). Each row is obtained from the row immediately above it by operations involving $\{c_k\}$ and $\{d_k\}$, and is shown in the figure as applying the filters C and D repeatedly, which for a Haar representation are $C = \left\{\frac{1}{\sqrt{2}}, \frac{1}{\sqrt{2}}\right\}$ and $D = \left\{\frac{1}{\sqrt{2}}, -\frac{1}{\sqrt{2}}\right\}$.

A subset of N coefficients which correspond to an orthonormal basis could be selected, and each choice gives a particular basis. The important thing to be noticed here is that a

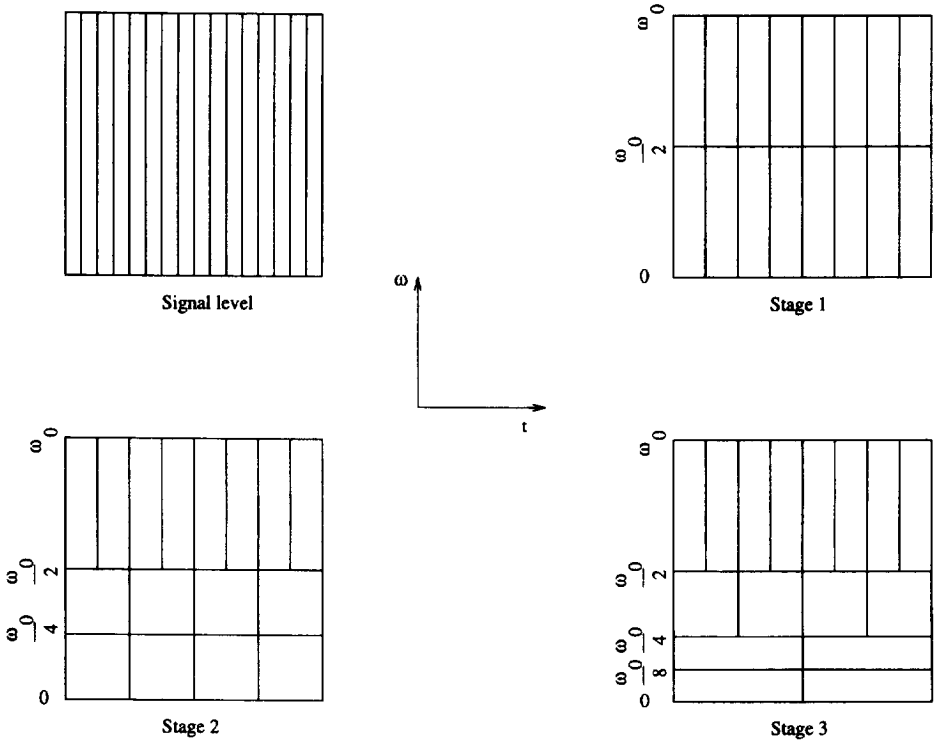

Fig. 2. Various stages of partitioning of the time–frequency plane in a wavelet decomposition.

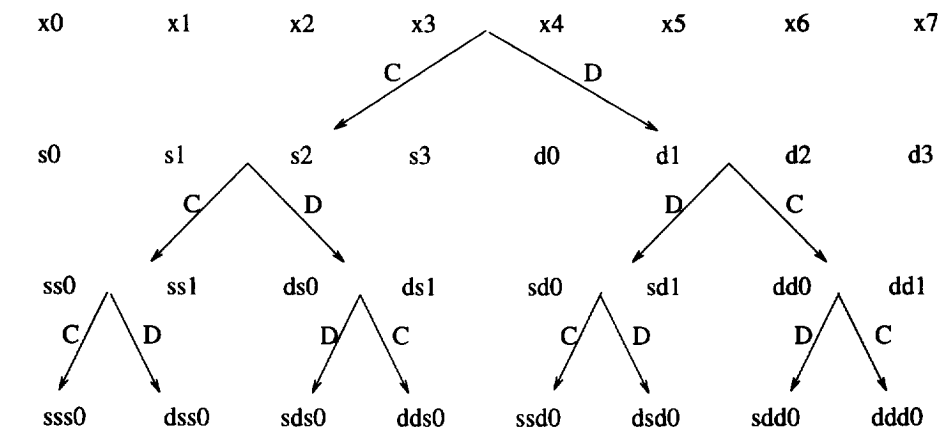

$$s0 = (x0 + x1)/2^{1/2} \qquad s1 = (x2 + x3)/2^{1/2} \qquad d0 = (x0 - x1)/2^{1/2} \qquad d1 = (x2 - x3)/2^{1/2}$$

$$ss0 = (s0 + s1)/2^{1/2} \qquad ds0 = (s0 - s1)/2^{1/2} \qquad sd0 = (d0 - d1)/2^{1/2} \qquad dd0 = (d0 + d1)/2^{1/2}$$

Fig. 3. A rectangle of wavelet packet coefficients (adapted from Wickerhauser (1991)).

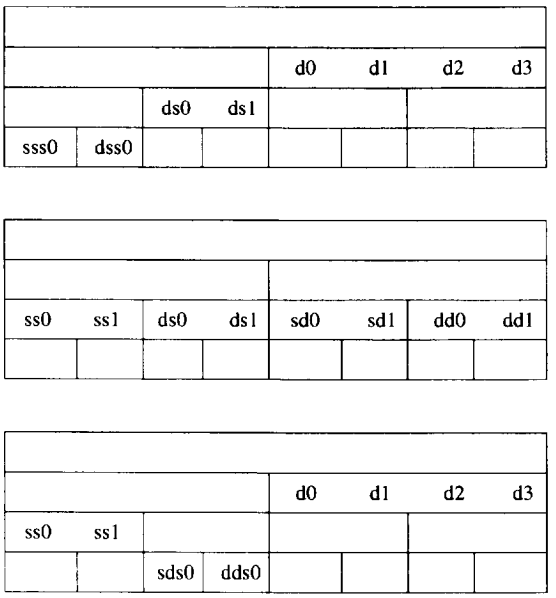

WAVELET BASIS
Only the high frequency component (right end) is retained and the low frequency (left) is further decompo--sed.

BEST LEVEL BASIS
The components at one level of dec--omposition are retained, based on which level has the least number of coefficients carrying most of the en--ergy.

ARBITRARY ORTHONORMAL BASIS
The components are selected so that the frequency axis is partitioned in a data-adaptive way.

Fig. 4. A few combinations yielding orthonormal bases (adapted from Wickerhauser (1991)).

wavelet basis is just one of the ways of choosing this subset. Choosing elements from a single level is analogous to a short-time Fourier transform. The last-level selection results in a basis analogous to the Fourier basis, and the zero-level selection is similar to the standard basis (superposition of Dirac deltas). Thus, in summary, all three bases discussed above can be obtained from a wavelet packet tree. A few possibilities including those mentioned above are shown in Fig. 4.

Thus we have a huge library of orthonormal bases, each capable of representing a signal in its own right. We try to extract a basis which is the best in terms of providing a good contrast between low and high energies. A good choice for an objective function (also called the cost function) is entropy, as entropy = − information. The Shannon–Weaver entropy of a sequence $x = \{x_j\}$ is defined as $H(x) = -\sum_j p_j \log p_j$ if $p_j \neq 0$ and $H(x) = 0$ if $p_j = 0$, where $p_j = (|x_j|^2/\|x\|^2)$. A known aspect of this cost function is that $\exp H(x)$ is proportional to the number of coefficients needed to represent the function to a fixed mean square error. The basis so obtained by minimizing entropy is given the name best basis (Wickerhauser, 1991).

The rectangles in the time–frequency plane defined by $k2^{-j} \leq t < (k+1)2^{-j}$ and $n2^j \leq \omega < (n+1)2^j$ are associated with the wavelet packet $2^{j/2}\omega_n(2^j t - k)$, where k corresponds to position, n to frequency and j to scale. In words, position refers to the center of the basis functions, scale refers to the width of the support of the basis functions, and frequency refers to the number of oscillations over this support of the basis functions (or equivalently the center of the Fourier transform of the basis function). The best basis of wavelet packets tries to maximize the energy captured by each rectangle. This ensures that when the signal is expanded in the best basis all or most of its energy is captured with the fewest number of basis elements (or equivalently coefficients).

To sum up, wavelet packets provide a much more flexible and data-adaptive decomposition of a signal and are preferable for the following reasons (Meyer, 1993): (1) Daubechies' orthogonal wavelets are a special case of wavelet packets; (2) wavelet packets are organized naturally into collections and each collection is an orthonormal basis for $L^2(R)$; thus, one can compare the advantages and disadvantages of the various possible decompositions, based on a chosen objective function, and represent the signal in an optimal way. In addition, as observed above, most of the energy can be captured by very few coefficients by a judicious choice of the objective function.

2.1. Measures to interpret the time–frequency plots

2.1.1. Best basis spectrum

The time–frequency–energy plots of the best basis include information about scales, too. As mentioned above, it is important to note that there is a fundamental difference in the wavelet transform and the wavelet packet transform domain in terms of the way one looks at the entity scale. In the former case, scale = (frequency)$^{-1}$ i.e. every scale is spanned by a one-period wave. In the latter case, scale $\neq$ (frequency)$^{-1}$, i.e. every scale (support of the analysis window) is spanned by multiple period waves (one-period wave to Nyquist-period waves). Thus the partition of the time–frequency plane by the wavelet packet best basis (WPBB) gives us information on how much energy is present in a frequency band (i.e. the sum of the squares of the best basis coefficients associated with that frequency band) and over length scales (in time) that best represent that frequency band. Indeed, the tiling across a particular frequency band, i.e. the size of the Heisenberg rectangles, directly reflects on the scale to which the decomposition has been done. To aid in the interpretation of the time–frequency–energy plots, we reduced the plots to two one-dimensional plots. The first plot (energy vs. frequency) captures the energy encompassed in various frequency bands (analogous to the Fourier spectrum), and is what we define as the best basis spectrum (referred to below as the BBS).

The BBS is computed in the same way as the Fourier or the discrete wavelet spectrum, the only difference being that, in the best basis scenario, we have frequency bands which have been selected in a data-adaptive way, i.e. the distribution of energy into different frequency bands is done in an adaptive fashion, unlike in the Fourier or the discrete wavelet transform domain. The BBS cannot by itself describe completely the time–frequency–energy plots, thus calling for the definition of another measure that can complement the information provided by the BBS.

2.1.2. Frequency persistence spectrum

Wavelet packets can choose to characterize a frequency with a persistent amplitude (and also phase) by a tiling (Heisenberg rectangle) that is elongated in the time domain (equivalently good localization in the frequency domain), such that we have multiple periods over a particular length scale (note that this is in contrast to the wavelet transform, where we have one period per length scale). To quantitatively characterize such a property of the wavelet packets, we introduce a measure, $2^{\text{level}} \times f$, which is the number of periods corresponding to the frequency f over a length scale (length of the Heisenberg rectangle in time) which is equal to 2^{level} (level here means the level of decomposition, i.e. the zeroth

level corresponds to the signal itself and the last level corresponds to a Fourier-like representation of the signal). Such a measure directly reflects the persistence (length scale) of the frequency f in the phenomenon. Hence we call the plot of (2^{level} × frequency) vs. frequency as the frequency persistence spectrum (FPS). The quantity (2^{level} × frequency) remains a constant with frequency for a wavelet basis. This constant could be one or two, depending on the representative frequency chosen for the frequency band (lower or upper end) as elaborated below. In Fig. 2, different stages of a wavelet decomposition are shown: at Stage 3, the frequency bands (normalized by the Nyquist frequency, i.e. ω_0) are [1/8,1/4], [1/4,1/2] and [1/2,1] and the associated levels of decomposition are three, two and one, respectively. If one were to choose the lower end of each frequency band as the representative frequency, i.e. 1/8, 1/4 and 1/2, then the FPS would be $2^3 \times (1/8)$, $2^2 \times (1/4)$ and $2^1 \times (1/2)$, respectively, and thus the constant is unity. On the other hand, if we were to take the upper end as the representative frequency, then the associated FPS would be $2^3 \times (1/4)$, $2^2 \times (1/2)$ and $2^1 \times (1)$, and hence the constant is two. For our analysis, we chose the upper end as the representative frequency. For the rest of the paper, when we refer to frequency in the FPS or BBS, it is a normalized (by Nyquist frequency) frequency.

Thus, the FPS of a signal can give a qualitative and also a quantitative idea of how different the best basis for the signal is from the wavelet basis. The quantitative idea comes from the fact that the FPS gives us the level (or equivalently scale) to which the decomposition has been carried out to localize a particular frequency. In fact, the level can be computed as

$$\text{level} = \log_2 I \tag{4}$$

where I is the intercept of the line $L = 2^{level}$ on the (2^{level} × frequency) axis in the FPS (ordinate positioned at abscissa of unity in a log–log plot). For instance, let us consider Fig. 5, in which the FPS and BBS for a signal have been shown in a log–log domain. The horizontal broken line in the FPS at (2^{level} × frequency) = 2 (as mentioned above) corresponds to the wavelet basis. Each broken line represents one level of decomposition (only a few levels are shown in the figure). It is important to note that each frequency has a unique level of decomposition associated with it (this follows directly from the fact that we are dealing with a basis). Furthermore, it is worth mentioning that two different frequency bands could have the same level of decomposition, which would not be possible with a wavelet basis. From that figure, for instance, if we were to take a frequency in the high-frequency region (frequency between 10^0 and 10^{-1}), the value of (2^{level} × frequency) for the best basis is higher than that for the wavelet basis. This means that the level to which the decomposition has been done is greater in the best basis, implying a better localization of that frequency (correspondingly, an elongated rectangle in the time direction) in the best basis framework. In other words, the best basis chose to represent that particular frequency by multiple period waves over a length scale = 2^{level}, which is not possible with the wavelet basis where a one-period wave is used to represent the frequency over the length scale mentioned above. This feature of the best basis is important when one wishes to study the presence of persistent high-frequency (amplitude and phase remain the same for a time period longer than the period of the oscillation) features in a phenomenon. On the other hand, if we were to consider a frequency in the low-frequency region (frequency between 10^{-3} and 10^{-4}), the quantity (2^{level} × frequency) is same in the best basis as in the wavelet

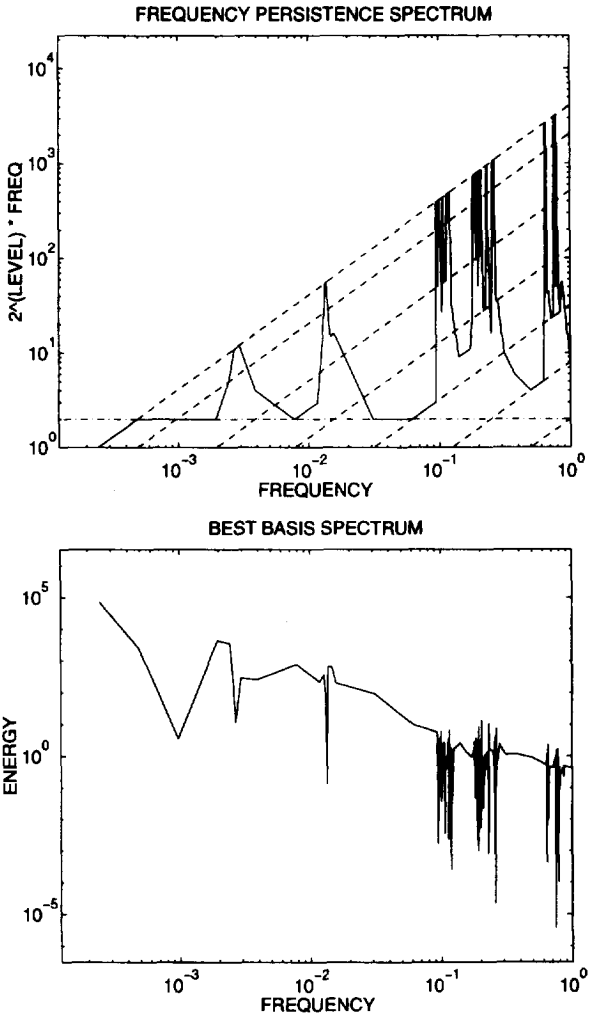

Fig. 5. Schematic representation of the frequency persistence spectrum (FPS—top) and best basis spectrum (BBS—bottom) for a signal, on a log–log scale. The broken lines correspond to levels of decomposition and can be computed using Eq. (4). The horizontal broken line corresponds to the FPS of a wavelet basis.

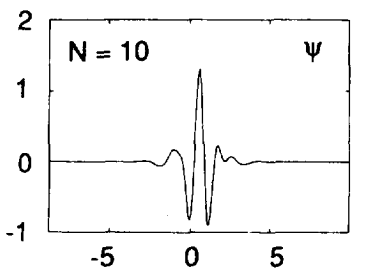

Fig. 6. Daubechies wavelet with 10 vanishing moments (adapted from Daubechies, 1992, p. 199).

basis, which indicates that the best basis chose to decompose a low frequency similar to the wavelet basis.

In summary, the two measures that we defined above are complementary and are both needed to fully characterize the time–frequency–energy plots, i.e. each of these measures alone is not sufficient. Having seen these two measures to interpret time–frequency–energy plots, we turn our attention to the analysis of high-resolution temporal rainfall. The wavelet that was chosen for reporting the results of the analysis is one of the Daubechies' wavelets, D20, and is shown in Fig. 6. This wavelet has ten vanishing moments and thus is very smooth. This property, to start with, was thought to be useful for a process such as rainfall for the reason that rainfall exhibits considerable variability at all scales. However, the analysis with other wavelets (less smooth) yielded results that are not very different from each other. This naturally indicates the robustness of the technique, owing to weak dependence of the conclusions and results on the mother wavelet.

3. Analysis of temporal rainfall

3.1. Data description

The high-resolution temporal rainfall data that we have considered for analysis were collected at the Iowa Institute of Hydraulic Research (IIHR) over a period of 4 years (1989–1992), with specially calibrated instrumentation that allows high-resolution sampling. Further details about the instrumentation and other auxiliary data, such as wind speed, pressure, etc., collected at the same site have been given by Georgakakos et al. (1994).

We have data for seven storms that occurred during the period from May 1990 to April 1991. It is noted that the sampling interval of all the storms is 5 s, except for the storm on 2 December, which has a 10 s sampling interval. The maximum rainfall rates range from 10 to 120 mm h^{-1}, the average rain rates range from 0.38 to 3.9 mm h^{-1} and the coefficients of variation range from 0.75 to 2. The rainfall time series are shown in Figs 7–10.

For future reference, the following notation will be used:

Rain1:	Storm on 2 December 1990	Duration 26.9 h
Rain2:	Storm on 1 November 1990 (B)	Duration 11.7 h
Rain3:	Storm on 30 November 1990	Duration 12.2 h
Rain4:	Storm on 3 October 1990	Duration 9.8 h
Rain5:	Storm on 1 November 1990 (A)	Duration 9.3 h
Rain6:	Storm on 3 May 1990	Duration 9.3 h
Rain7:	Storm on 12 April 1991	Duration 2.9 h

The above notation has been chosen so as to remain consistent with the names of the events at the ftp site (which is used world wide). The original notation was made in the order of decreasing signal length. The two rainfall events that occurred on 1 November 1990 were labeled A and B in chronological order.

3.2. Time–frequency–scale analysis

Before we proceed with the discussion of the results, we briefly mention a few

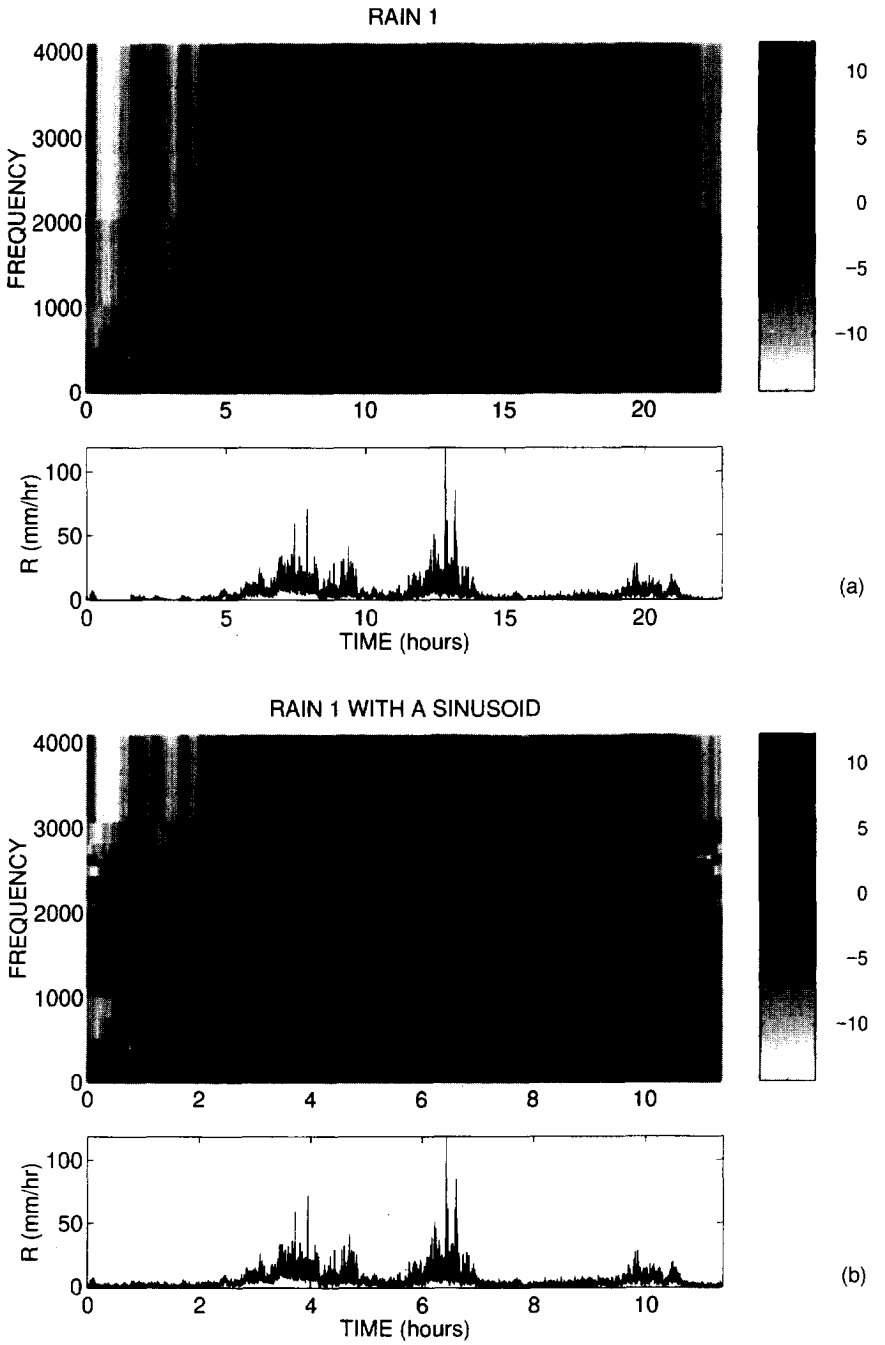

Fig. 7. Time–frequency–energy plot for (a) Rain1 (2 December 1990) and (b) Rain1 with a sinusoid of frequency 2250 units. The gray scale represents energy, on a log scale. Analysis was done with a Daubechies 20 wavelet.

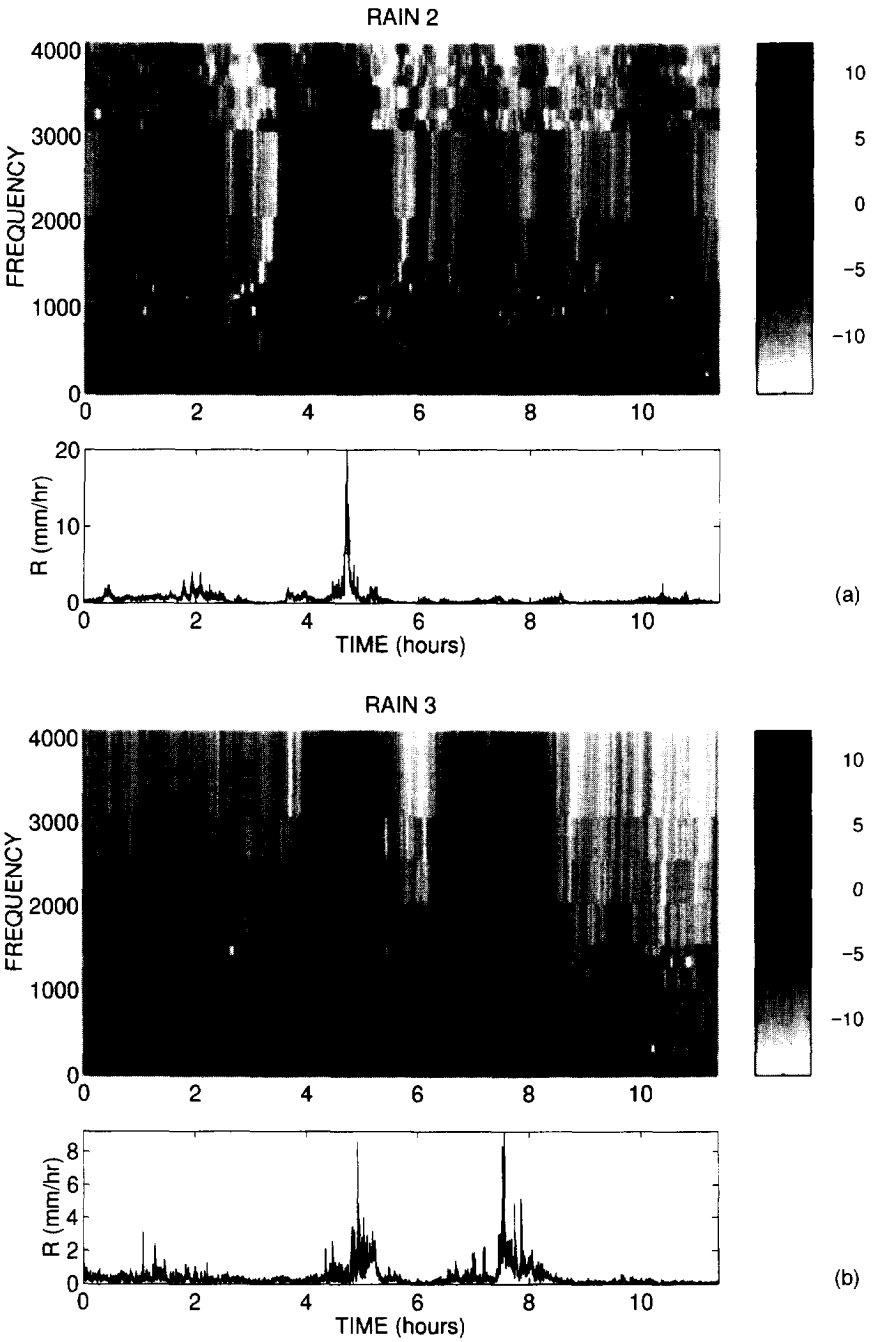

Fig. 8. Same as Fig. 7, but for (a) Rain2 (1 November 1990 (B)) and (b) Rain3 (30 November 1990).

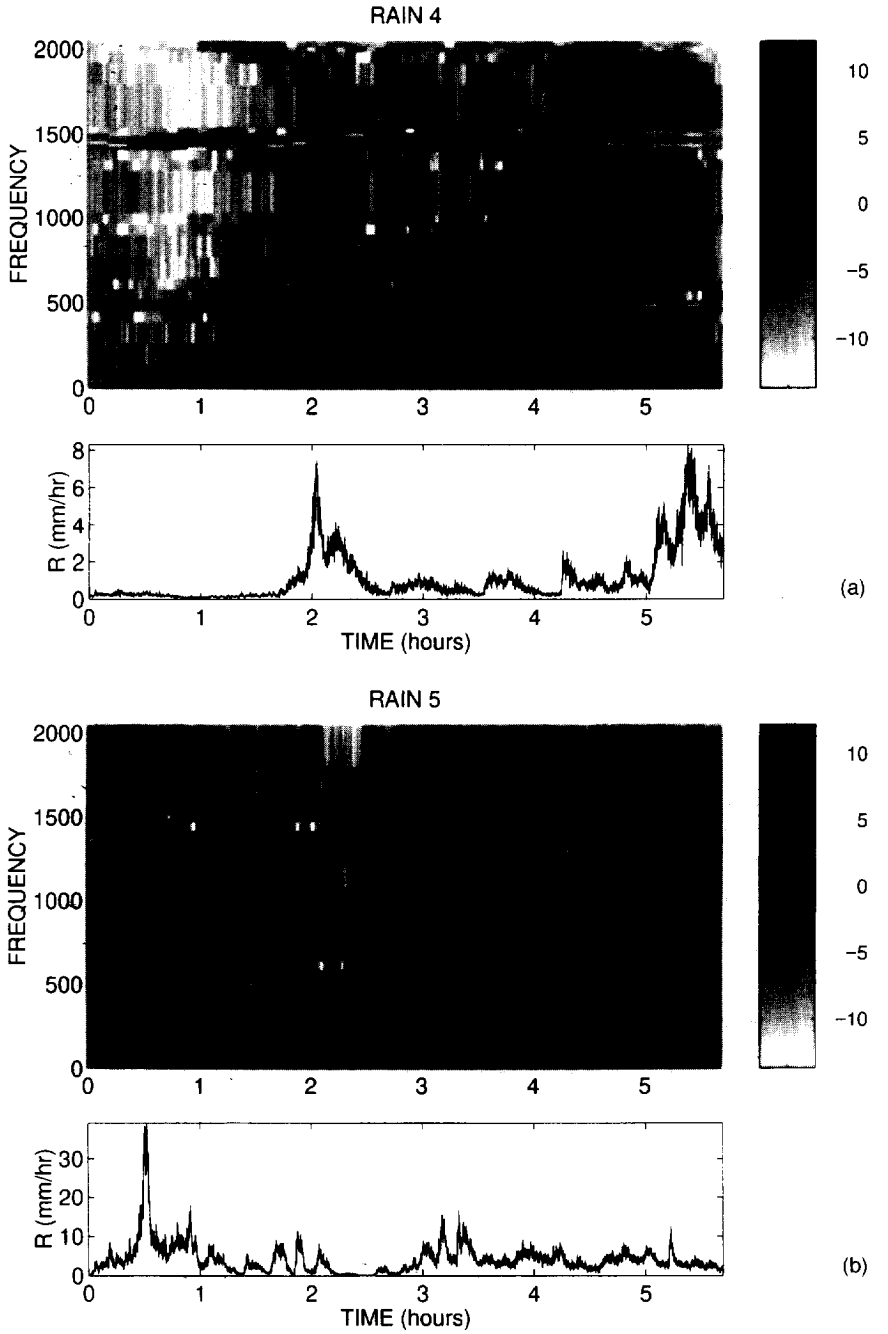

Fig. 9. Same as Fig. 7, but for (a) Rain4 (3 October 1990) and (b) Rain5 (1 November 1990 (A)).

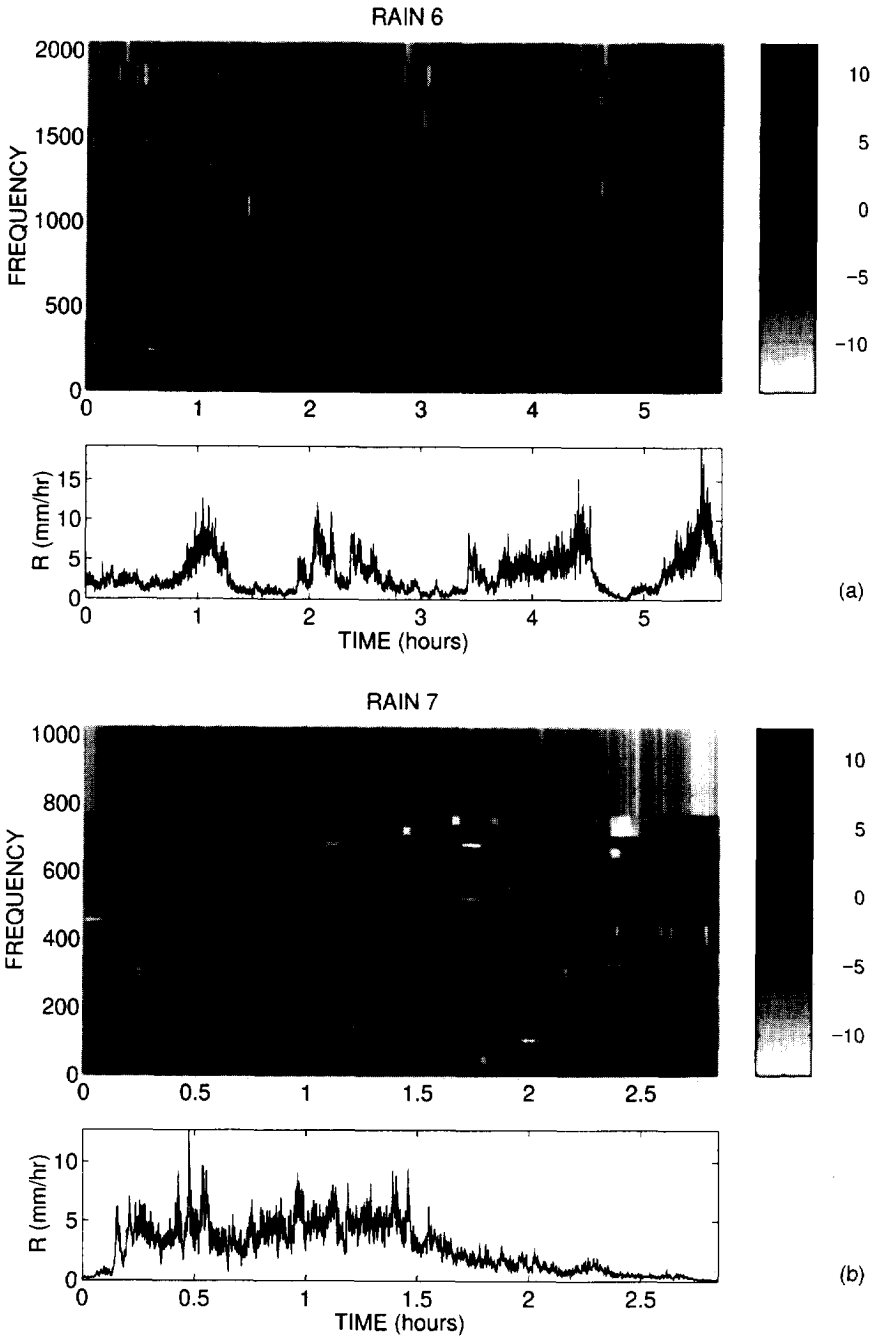

Fig. 10. Same as Fig. 7, but for (a) Rain6 (3 May 1990) and (b) Rain7 (12 April 1991).

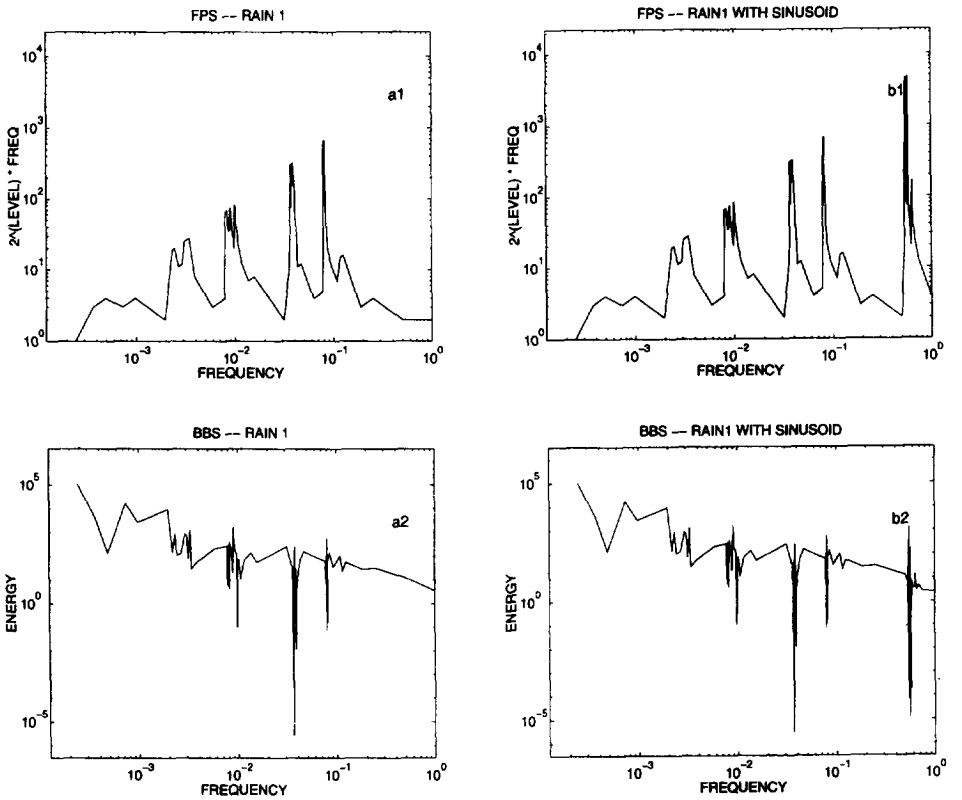

Fig. 11. Frequency persistence spectrum (FPS) and best basis spectrum (BBS) for (a) Rain1 (2 December 1990) and (b) Rain1 superposed with a sinusoid of frequency 2250 units.

computational aspects of our analysis. An important consideration in the wavelet packet framework is that the signal length be necessarily a power of two. Towards this end, for Rain1, Rain2 and Rain3, which had more than 8192 points, the signal length was chosen to be 8192. On the other hand, for Rain4, Rain5 and Rain6, which had about 6600 points, we chose the signal length to be 4096 instead of padding with zeros to make the signal length 8192. For Rain7, the part of the signal amounting to 2048 points was chosen as the signal to be analyzed (out of 2060 points). Also in the time–frequency–energy plots (Fig. 7 and Fig. 10), the energy values (squares of the amplitudes of the best basis coefficients) have been plotted on a log scale to see contrast in the energy distribution across frequencies. An additional aspect worth mentioning in these plots is that the frequency axis varies from zero to $\frac{N}{2}$, (N is the signal length), and does not represent the actual frequencies. In addition, in both the FPS and BBS plots that depict the measures quantifying the time–frequency–scale representations (Figs 11–14), the frequency is normalized by $\frac{N}{2}$.

First, as the cost function that is minimized is the entropy, it implies that the time–frequency plots will provide maximum contrast in energies. Second, features of a process are reflected not only in the amplitudes of the coefficients but also in the structure of the chosen basis, in other words, the way of tiling the time–frequency plane. If the signal were

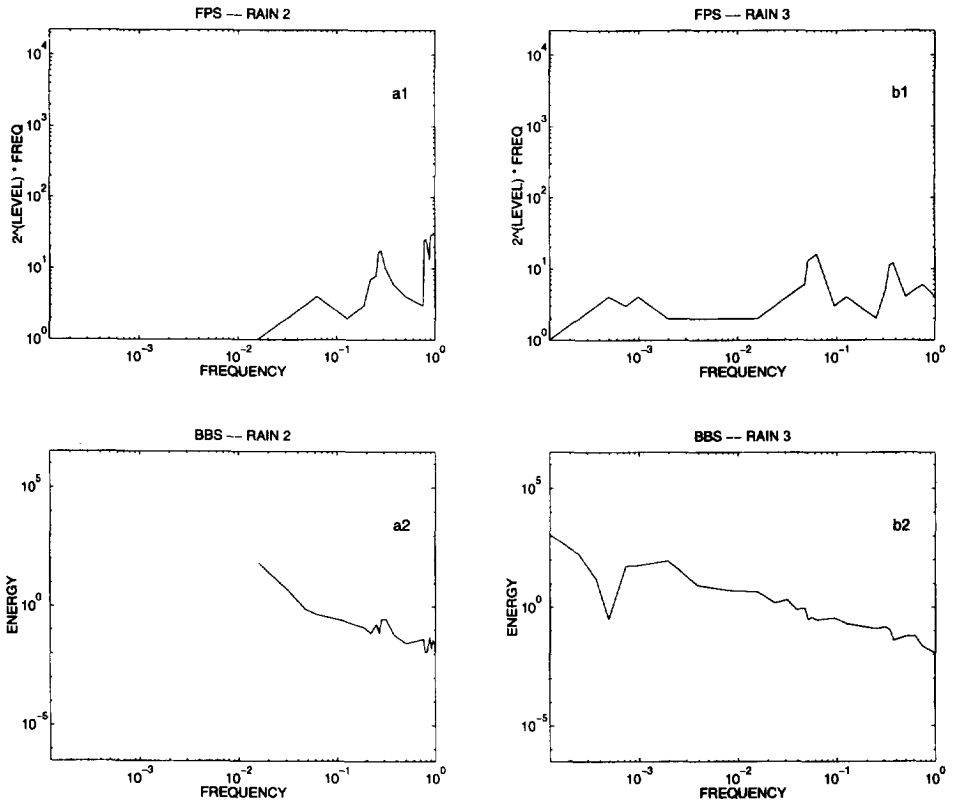

Fig. 12. Frequency persistence spectrum (FPS) and best basis spectrum (BBS) for (a) Rain2 (1 November 1990 (B)) and (b) Rain3 (30 November 1990).

to have persistent frequencies (frequencies which preserve their amplitude and phase over a period of time which is significantly longer than the corresponding wavelength), then the best basis selected from the wavelet packet family reveals such a feature as elongated rectangles in the time direction, at those frequencies.

As rainfall is a complicated process, it is impossible to know a priori if any persistent frequencies are present. To check how and if wavelet packets find the presence of a persisting frequency, we imposed a sinusoid (of amplitude unity and frequency 2250 units, or a normalized frequency of (2250/4096), i.e. 0.55) over the whole length on a rainfall data set (Rain1). The time–frequency plot for the rain and the rain with the imposed sinusoid are shown in Fig. 7(a) and (b), respectively. It is evident from these figures that, in the latter case, there is an elongated rectangle at the appropriate frequency, which reveals the presence of a persistent frequency (imposed sinusoid). Correspondingly, in the FPS (Fig. 11(b1)), we see a spike at a frequency of 0.55 (the frequency of the superposed sinusoid), which is not present in the frequency persistence spectrum of the original signal, i.e. Rain1 (Fig. 11(a1)). Also evident is the peak in the best basis spectrum at the same frequency (indicating the presence of a 'feature' with considerable energy). The fact that wavelet basis is a rigid basis prevents it from indicating the presence of

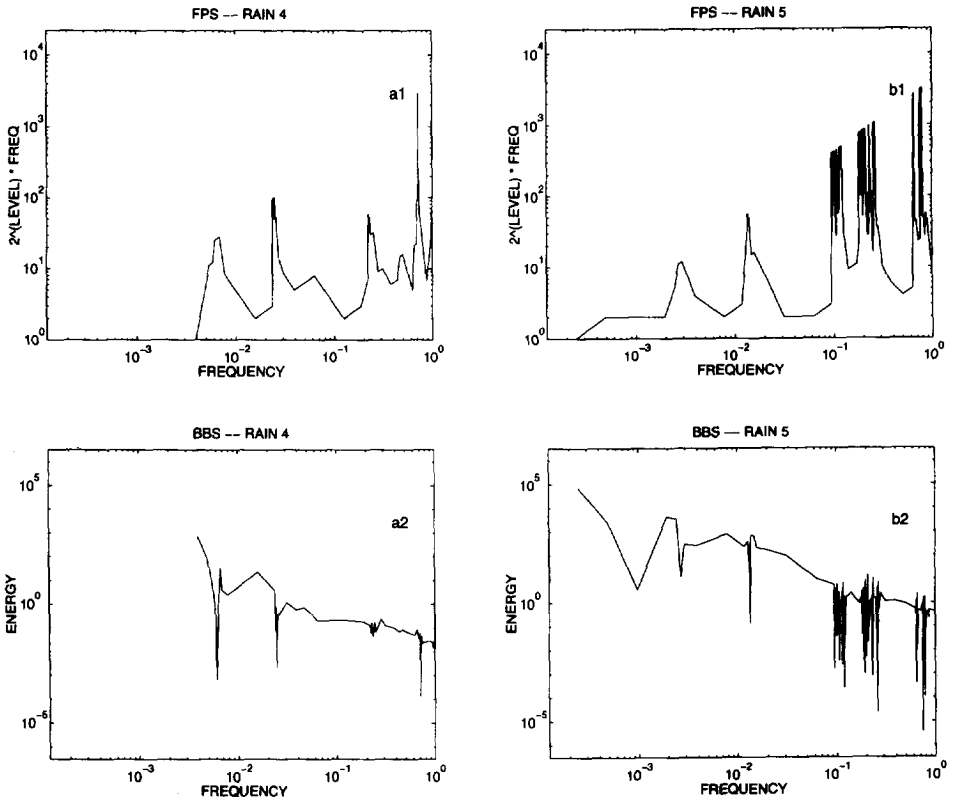

Fig. 13. Frequency persistence spectrum (FPS) and best basis spectrum (BBS) for (a) Rain4 (3 October 1990) and (b) Rain5 (1 November 1990 (A)).

persistent frequencies, if any. Keeping in mind this potentially powerful capability of the wavelet packet best basis (adaptive tiling), let us look at the time–frequency representations in the wavelet packet best basis domain of different rainfall events.

Figs 8–10 show the wavelet packet best basis phase-space (time–frequency–energy) plots and the associated spectra (best basis and frequency persistence spectra) for the events Rain2–Rain7. One striking feature from the time–frequency plots is the drastic difference in tiling in some rainfall events compared with the others. For instance, if we compare the plots for Rain1 and Rain4 (or Rain5), we see an intriguing difference in tiling. For Rain1, the top part of the plot, which corresponds to the decomposition of the high-frequency bands, is similar to the wavelet decomposition, whereas that for Rain4 is completely different from the wavelet decomposition. We emphasize here the fact that with a wavelet decomposition it is impossible to see such differences, although the concentration of high- and low-activity regions in time will be similar to that indicated by the wavelet packet best basis decomposition. Indeed, the difference seems similar to the case of the difference between Rain1 and Rain1 with the superposed sinusoid. Hence one can conclude (with a reasonable amount of certainty) that elongated rectangles in the time–frequency plot for Rain4 (and Rain5) indicate the presence of persistent frequencies whose

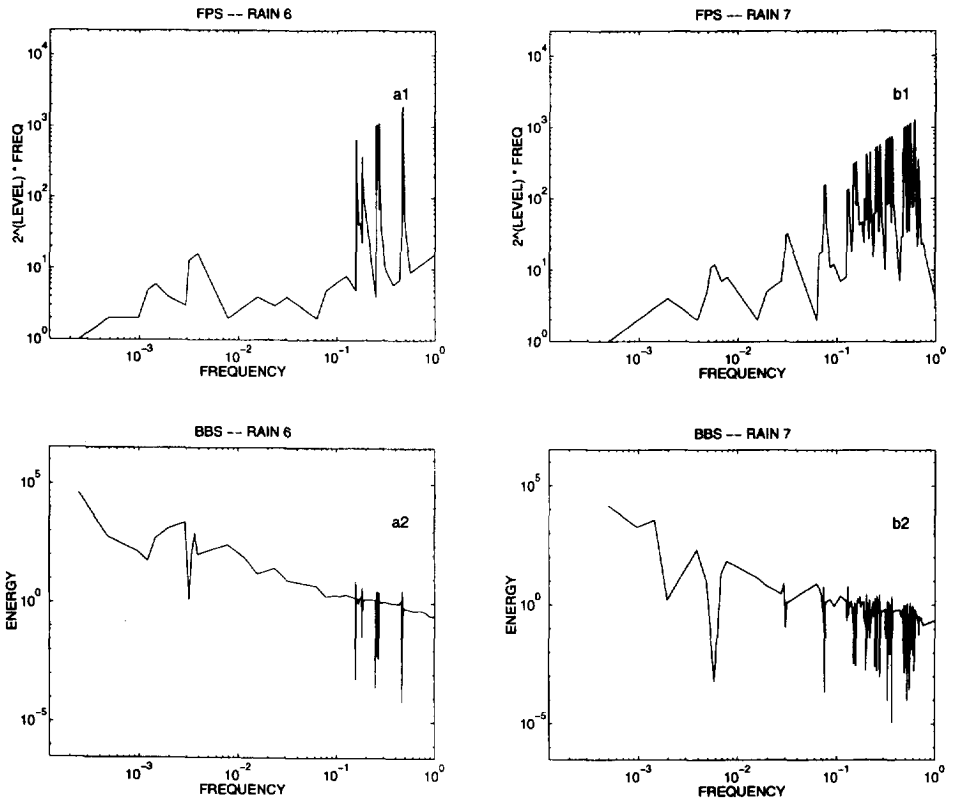

Fig. 14. Frequency persistence spectrum (FPS) and best basis spectrum (BBS) for (a) Rain6 (3 May 1990) and (b) Rain7 (12 April 1991).

associated energy is obtained from the BBS. The wavelength (referred to here as EW (for equivalent wavelength)) corresponding to a particular frequency f is computed as $\lambda = \delta t \cdot N/f$, where δt is the sampling interval and N is the signal length. In the time–frequency–energy plot for Rain1 (sampling interval 10 s), the frequencies between 500 (EW = 160 s) and 4000 (EW = 20 s) have been localized very well in time. In other words, this indicates the presence of short-lived structures of time scales (durations) of the order of 20–160 s (in the frequency band 500–4000). The FPS indicates that the level of decomposition corresponding to these frequencies is close to zero, implying that the localization of these frequencies in time is good (which is expected, as the FPS only quantifies the time–frequency–energy plot). Referring again to the FPS (Fig. 11(a1)), frequencies which have values around 125 (EW = 640 s) and 350 (EW = 200 s) (normalized frequencies are 0.03 and 0.09) have been localized in the frequency direction very well, which is indicated by peaks at those points. The level corresponding to these frequencies is 13, which is the last level of decomposition and corresponds to a time scale of about 20 h. On the other hand, we note that the BBS (Fig. 11(a2)) indicates relatively less energy at these frequencies. This means that a structure with a very high degree of persistence, relatively low frequency and relatively low energy does exist in the

process. It is conjectured that this corresponds to the stratiform portion of the rainfall signal, whereas the high-energy short-lived structures (features) correspond to the convective portion of the rainfall event. Further analysis and data are needed to corroborate this conjecture and implement it for convective vs. stratiform rainfall separation.

In Rain2 (sampled at 5 s), which has just one burst of activity, it is evident from the FPS (Fig. 12(a1)) that there is almost no persisting structure over a time scale of more than about 4–5 min (the maximum intercept on the (2^{level} × frequency) axis is about 60, which, using the expression for the level from Eq. (4), leads to a level of decomposition equal to six, which in turn corresponds to about 320 s). The fact that this rainfall event had only one really strong burst of activity suggests that it should have been due to a short-lived structure; the best basis corroborates this aspect and also provides us with a quantitative estimate of the length scale of this structure as equal to about 4–5 min.

Rain3 (sampled at 5 s) looks similar to Rain1, in terms of having two high-activity regions. The decomposition of Rain3 in the best basis framework is shown in Fig. 8(b). The high- and low-activity regions have been depicted fairly well. The BBS indicates an almost power-law behaviour. From the FPS shown in Fig. 12(b1), it is evident that there is no particular length scale for the process, except for the really low frequencies (for instance, the process average), where the analysis shows the presence of a scale of length equal to the signal length, which is 8192 points or 12 h. This was expected, considering the fact that rainfall is a positive mean process and the mean has the highest energy, which is evident from the BBS (Fig. 12(b2)). In addition, the lack of presence of a predominant scale in the process is confirmed by the BBS, which shows a fairly good linear behaviour in the log–log domain (a fact worth mentioning here is that the Fourier power spectrum showed a similar behaviour).

Referring to the plots for Rain4, Rain5 and Rain6 (each of which was sampled at 5 s), which are shown in Fig. 9(a), (b) and Fig. 10(a), respectively, it seems that Rain5 seems to have many persistent structures of the same length scale (from 4–6 h), but over a different range of frequencies (between 500 (EW = 80 s) and 1500 (EW = 25 s)), i.e. over the same length scale, we have different number of periods. Again from the BBS (Fig. 13(b2)), the energies corresponding to those frequencies are very low (dips at those frequencies).

Rain7, as is evident from the signal, does not have any short bursts of energy, and from what has been seen until now, we should expect many persistent structures. Indeed, the time–frequency–energy plot (Fig. 10(b)) and the FPS (Fig. 14(b1)) show this feature. This indicates that the predominant time scale is between 1.2 and 3 h, which is the duration of the storm. There is more variation in the first half of the storm compared with the second half. This aspect is manifested in the time–frequency–energy plot as the presence of high frequencies (between 800 (EW = 15 s) and 1000 (EW = 40 s)) with relatively more energy in the first half compared with the second half (as shown by the contrast in the gray scale).

3.3. Rainfall 'signal' compression

Another by-product of the wavelet packet decomposition, which was mentioned in the Introduction, is the aspect of compression. Table 1 shows the proportion of energy (relative to the original signal) captured by the signal (rainfall) reconstructed from a number of (highest) coefficients out of the complete best basis.

Table 1
Percentage of energy captured by the highest (in absolute value) N coefficients of the best basis

Signal	Signal length	Number of coefficients (highest)	Energy captured (%)
Rain1	8192	50	81
		500	95.4
		1500	99
Rain2	8192	50	82.6
		500	99.3
		1500	99.9
Rain3	8192	50	86.4
		500	97.5
		1500	99.5
Rain4	4096	50	97.3
		250	99.1
		750	99.8
Rain5	4096	50	95.8
		250	98.7
		750	99.5
Rain6	4096	50	94.5
		250	97.8
		750	99.3
Rain7	2048	10	93
		50	96.2
		100	98

From Table 1 it is evident that with a very few (relative to the size of the signal) best basis highest coefficients, almost all of the energy is captured. Fig. 15 shows Rain1 reconstructed with the highest 50 and 500 wavelet packet best basis coefficients. Fig. 16 shows the percentage of energy captured by N maximum best basis coefficients, where N varies from ten to 1000 coefficients, for Rain1. Although not explored here, the compressibility feature of wavelet packet best basis can be useful for storage of large remotely sensed data sets or even for non-parametric comparison or simulation of hydrologic processes.

4. Conclusions

From the time–frequency–scale analysis we have performed on the high-resolution temporal rainfall, we draw the following conclusions:

1. Revealing the presence of time–frequency–scale features in a signal is important for understanding the structure of a signal in general, and rainfall in particular. Indeed, persistent high-frequency features may reflect the presence of a periodic (repeating) process in the rainfall-producing mechanism, e.g. a periodicity in the uplifting vertical motion of the atmosphere within the precipitating cloud. Also, knowledge of the presence of such structures, with the associated energy distribution among scales and frequencies, is useful information which can be used in building energy cascading

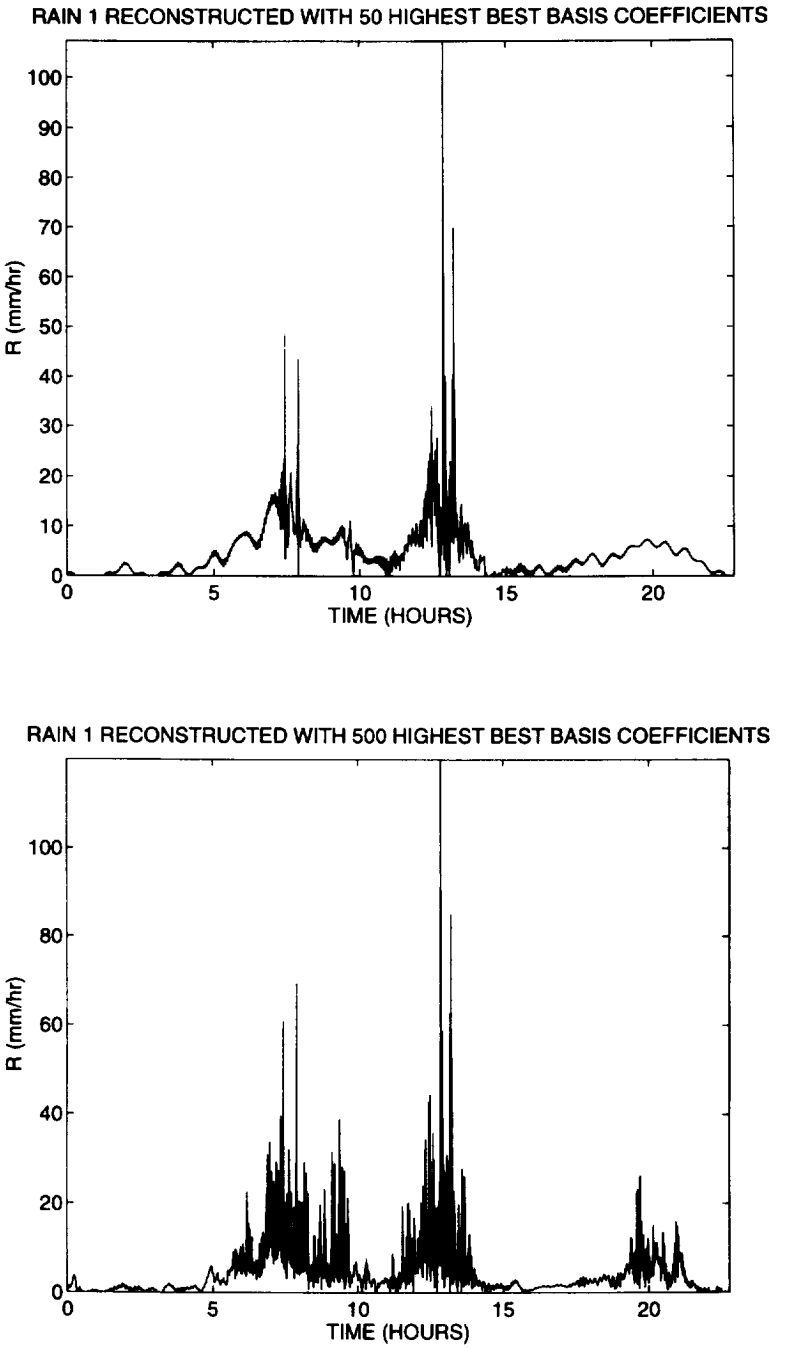

Fig. 15. Rain1 reconstructed from 50 (top) and 500 (bottom) highest best basis coefficients.

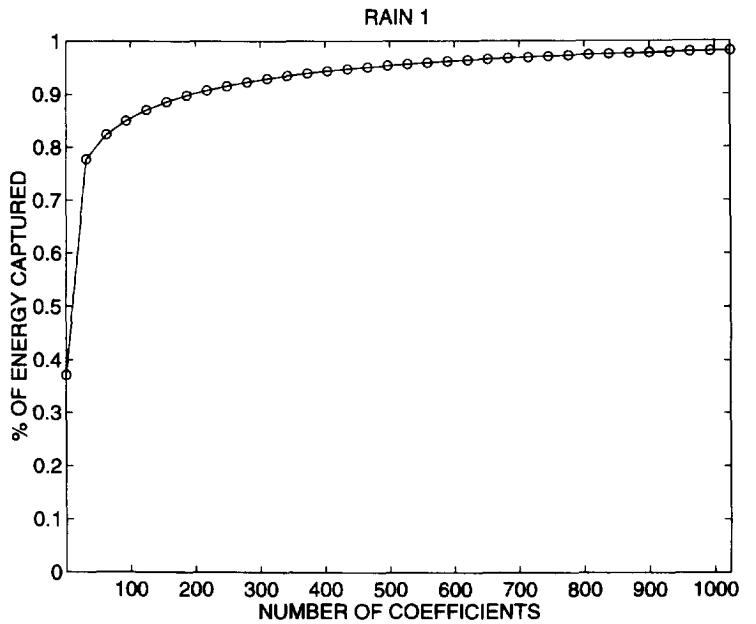

Fig. 16. Percentage of energy captured by N highest best basis coefficients for Rain1. Similar plots are found for Rain2–Rain7.

models of temporal rainfall. The tool used in our analysis is wavelet packets, and it is evident that they are versatile and capture time–frequency–scale features better than the short-time Fourier (STFT) or wavelet transforms, because they are capable of representing a signal in a data-adaptive way. In addition, the wavelet packet family includes both the short-time Fourier and wavelet transforms and thus if either of the latter were the best representation for the signal, the best basis approach would find it.

2. Our analysis can have several implications for multiscale rainfall modeling and, in particular, in identifying what type of cascading models are most appropriate for temporal rainfall (see also Cârsteanu and Foufoula-Georgiou (1996)). Wavelet decomposition is consistent with the assumption of multiplicative cascades currently used for modeling rainfall (e.g. Lovejoy and Schertzer, 1987; Gupta and Waymire, 1990; Over and Gupta, 1994), which split the energy in the same way across scales. It is possible, as shown here, that the distribution of energies changes across scales, resulting in the need to explore other types of cascading models. As wavelet packets are data-adaptive, they can possibly show such cascading structures and aid in model building (e.g. see Farge et al. (1992) for similar ideas in two-dimensional turbulence).
3. Our analysis can lead to valuable interpretations regarding the importance of long-term (persisting) and short-lived structures in rainfall. We conjecture that structures which persist, but have relatively low energy in a rainfall event, indicate the presence of a stratiform portion of rain. A storm in general occurs in a three-dimensional environment, and the vertical motion (and distribution of heating) of the atmosphere varies

drastically within the stratiform and convective parts of the storm. Vertical motion in the convective parts is very active, whereas it is almost non-existent in the stratiform parts. It is hence of considerable interest to separate the stratiform and convective components in rainfall, especially for water budget studies in the precipitating clouds. Based on the results of the one-dimensional study presented here, we envision that the analysis tool we used, i.e. the wavelet packets, can be successful in a two-dimensional framework, to separate the convective and stratiform components of a storm. In addition, considering the fact that wavelet packet best basis is selected in a data-adaptive way, analysis using wavelet packets would be a more objective approach than the traditional thresholding techniques or the recently developed eigenvalue technique (Bell and Suhasini, 1994) for separating convective and stratiform precipitation. The convective component of a rainfall event is usually the one with high energy and is also a highly fluctuating phenomenon (e.g. a sudden and heavy downpour). Such a feature can easily be detected by wavelet packets as the high-frequency short-lived components. The stratiform component, being the more subdued component, can be seen in the wavelet packet best basis regime as a persisting structure with considerably lower energy (it could be of low or high frequency as demonstrated).

Our analysis is thus seen as a first step in the direction of seeking to unravel frequency–scale–energy information from the rainfall process and use this information for modeling and inference (see also the more recent study by Kumar (1996)). Analysis of temporal rainfall in regimes other than the midwestern regime used in this work is needed to strengthen the physical interpretation and significance of the unraveled structures. Finally, application to two-dimensional radar-observed rainfall fields is expected to be more interesting and illustrative, as stratiform and convective parts of the storm are more easily distinguishable.

Acknowledgements

This research was partially supported by NSF (Grant EAR-9117866), NASA (Grant NAG 5-2108) and NOAA (Grant NA46GP0486). Helpful comments from Alin Cârsteanu and Victor Sapozhnikov are greatly appreciated. The authors also acknowledge the support of the Minnesota Super Computer Institute.

References

Bell, T.L. and Suhasini, R, 1994. Principal modes of variation of rain-rate probability distributions. J. Appl. Meteorol., 33: 1067–1078.

Cârsteanu, A. and Foufoula-Georgiou, E., 1996. Assessing dependence among weights in a multiplicative cascade model of temporal rainfall. J. Geophys. Res. Atmos., in press.

Daubechies, I., 1992. Ten Lectures on Wavelets. SIAM, Philadelphia, PA.

Farge, M., Goirand, E., Meyer, Y., Pascal, F. and Wickerhauser, M.V., 1992. Improved predictability of two-dimensional turbulent flows using wavelet packet compression. Fluid Dyn. Res., 10: 229–250.

Foufoula-Georgiou, E. and Guttorp, P., 1987. Compatibility of continuous rainfall occurrence models with discrete rainfall observations. J. Geophys. Res., 92(D8): 9679–9682.

Gabriel, K.R. and Neumann, J., 1962. A Markov chain model for daily rainfall occurrences at Tel Aviv. Q. J. R. Meteorol. Soc., 88: 90–95.

Georgakakos, K.P., Cârsteanu, A.A., Sturdevant, P.L. and Kramer, J.A., 1994. Observation and analysis of midwestern rainrates. J. Appl. Meteorol., 33(12): 1433–1444.

Gupta, V. and Waymire, E., 1990. Multiscaling properties of spatial rainfall and river flow distributions. J. Geophys. Res., 95(D3): 1999–2009.

Kumar, P., 1996. Role of coherent structures in the stochastic–dynamic variability of precipitation. J. Geophys. Res. Atmos., in press.

Kumar, P. and Foufoula-Georgiou, E., 1993a. A multicomponent decomposition of spatial rainfall fields: 1. Segregation of large and small-scale features, using wavelet transforms. Water Resour. Res., 29(8): 2515–2532.

Kumar, P. and Foufoula-Georgiou, E., 1993b. A multicomponent decomposition of spatial rainfall fields: 2. Self-similarity in fluctuations. Water Resour. Res., 29(8): 2533–2544.

Lovejoy, S. and Schertzer, D., 1987. Physical modeling and analysis of rain and clouds by anisotropic scaling multiplicative processes. J. Geophys. Res., 92(D8): 9693–9714.

Lovejoy, S. and Schertzer, D., 1990. Multifractals, universality classes and satellite and radar measurements of cloud and rain fields. J. Geophys. Res., 95: 2021–2034.

Mallat, S., A theory for multi-resolution signal decomposition: the wavelet representation. IEEE Trans. Pattern Anal. Mach. Intel., 11(7): 674–693.

Mallat, S., Multifrequency channel decomposition of images and wavelet models, IEEE Trans. Acoustics Speech Signal Analysis, 37(12): 2091–2110.

Meyer, Y., 1993. Wavelets: Algorithms and Applications. SIAM, Philadelphia, PA.

Olsson, J., Niemczynowicz, J. and Berndtsson, R., 1993. Fractal analysis of high-resolution rainfall time series. J. Geophys. Res., 98(D12): 23265–23274.

Over, T.M. and Gupta, V.K., 1994. Statistical analysis of mesoscale rainfall: dependence of a random cascade generator on the large-scale forcing. J. Appl. Meteorol., 33(12): 1526–1542.

Saito, N., 1994a. Simultaneous noise suppression and signal compression using a library of orthonormal bases and the minimum description length criterion. In: E. Foufoula-Georgiou and P. Kumar (Editors), Wavelets in Geophysics, Academic Press, San Diego, pp. 299–324.

Venugopal, V., 1995. Time–frequency–scale analysis of temporal rainfall. M.S. Thesis, Department of Civil Engineering, University of Minnesota, Minneapolis.

Waymire, E., Gupta, V.K. and Rodriguez-Iturbe, I., 1984. A spectral theory of rainfall intensity at the meso-β scale. Water Resour. Res., 20: 1453–1465.

Wickerhauser, V., 1991. Lectures on wavelet packet algorithms. Preprint, Department of Mathematics, Washington University, St. Louis.

Wickerhauser, V.M., Farge, M., Goirand, E., Wesfreid, E. and Cubillo, E., 1994. Efficiency comparison of wavelet packet and adapted local cosine bases for compression of a two-dimensional turbulent flow. In: C. Chui, L. Montefusco and L. Puccio (Editors), Wavelets: Theory, Algorithms and Applications, Academic Press, San Diego, pp. 509–531.